Decreased Interstitial Cell of Cajal Volume in Patients With Slow-Transit Constipation

CHONG–LIANG HE,*,‡ LARRY BURGART,§ LINAN WANG,§ JOHN PEMBERTON,‖ TONIA YOUNG–FADOK,‖ JOSEPH SZURSZEWSKI,*,‡ and GIANRICO FARRUGIA*,‡

*Department of Physiology and Biophysics, ‡Division of Gastroenterology and Hepatology, §Department of Pathology, and ‖Department of Surgery, Mayo Clinic, Rochester, Minnesota

Background & Aims: The cause of slow-transit constipation is incompletely understood. Recent observations suggest a central role for interstitial cells of Cajal in the control of intestinal motility. The aim of this study was to determine the volume of interstitial cells of Cajal in the normal sigmoid colon and in the sigmoid colon from patients with slow transit constipation. *Methods:* Sigmoid colonic samples were stained with antibodies to protein gene product 9.5, c-Kit, and α–smooth muscle actin. Three-dimensional reconstruction of regions of interest was performed using consecutive images collected on a laser scanning confocal microscope and ANALYZE software. *Results:* Volume of interstitial cells of Cajal was significantly decreased in all layers of sigmoid colonic specimens from patients with slow-transit constipation compared with normal controls. Neuronal structures within the colonic circular smooth muscle layer were also decreased. *Conclusions:* A decrease in the volume of interstitial cells of Cajal may play an important role in the pathophysiology of slow-transit constipation.

More than 4 million patients per year complain of frequent constipation.[1] Most cases are managed well with an increase in fiber intake and over-the-counter laxatives. A subset of patients with constipation, approximately 30% of patients seen for constipation in a tertiary referral center, have slow-transit constipation.[2] Slow-transit constipation is defined as decreased colonic transit as measured by radionucleotide techniques or radiopaque markers. Patients with slow-transit constipation respond poorly to an increase in dietary fiber and have variable responses to laxatives.[3] In patients in whom aggressive medical therapy for constipation fails, surgical therapy such as subtotal colectomy and ileorectostomy is a therapeutic option.[4]

The pathology of slow-transit constipation is not well delineated. There appears to be a defect in smooth muscle innervation in a subset of patients with slow-transit constipation; however, routine pathological studies of the resected colon are often unrevealing. Silver stains have shown a reduced number of argyrophilic neurons in some, but not all, surgical specimens.[5] A decreased number of neurofilaments in enteric ganglia has also been reported.[6] An increase, decrease, or no change in vasoactive intestinal polypeptide and substance P containing nerve fibers in colonic specimens from patients with severe constipation has been reported[7–9] as well as alterations in PACAP and nitric oxide synthase containing nerves.[7,8] A decrease in vasoactive intestinal polypeptide and nitric oxide synthase immunoreactive neurons has been described recently at the iliocecocolonic region in patients with idiopathic slow-transit constipation.[10]

The role of interstitial cells of Cajal (ICC) in coordinating intestinal motility has become more apparent in recent years. W/W^V mutant mice lack ICC at the level of the small intestinal myenteric plexus.[11,12] The small intestinal electrical slow wave is absent in these mice,[11,12] and small intestinal radiographs using barium show abnormal, slow, and uncoordinated motility.[13] Loss or structural alteration of ICC has been implicated in several disorders of human intestinal motility, including hypertrophic pyloric stenosis,[14] Hirschsprung's disease,[15–17] and intestinal pseudo-obstruction,[18–20] and also in ulcerative colitis.[21,22] The aims of this study were to establish normal values for total ICC volume in the human sigmoid colon and compare these values with data obtained from patients with severe slow-transit constipation requiring subtotal colectomy.

Materials and Methods

Procurement of human tissue was approved by the Institutional Review Board of the Mayo Clinic. All tissues were immediately snap-frozen after procurement and stored at −70°C until use. The investigator performing the data analysis was blinded to the clinical diagnosis (control vs. slow-transit constipation).

Abbreviations used in this paper: Cy, indocarbocyanine; ICC, interstitial cells of Cajal; LRSC, lissamine rhodamine; PGP, protein gene product; SMA, smooth muscle actin.

0016-5085/00/$10.00

Immunocytochemistry

Sigmoid colon samples were fixed with either 4% paraformaldehyde in 0.1 mol/L phosphate-buffered saline (PBS), pH 7.4, or Zamboni's fixative (Newcomer Supply, Middleton, WI) for 4 hours or held overnight at 4°C. Next, they were washed 3 times with 0.1 mol/L PBS, transferred to 30% sucrose in 0.1 mol/L PBS, and refrigerated for up to 24 hours until they were sectioned. Serial longitudinal, transverse, and horizontal sections (40–150 μm thick) were cut with a Cryostat (Miles Inc., Elkhart, IN), placed in spot plates, and flooded with 0.1 mol/L PBS with 0.3% Triton X-100 (Sigma Chemical Co., St. Louis, MO) and 5% normal donkey serum for 2 hours to permeabilize the tissue and to reduce background staining. Immunohistochemical staining was performed with the following antibodies: c-Kit rabbit polyclonal antibody (1:400 dilution; MBL, Nagoya, Japan); c-Kit goat polyclonal antibody (1:200 dilution; Santa Cruz Biotechnology, Santa Cruz, CA); protein gene product (PGP) 9.5 mouse monoclonal antibody (1:500 dilution; Biogenesis, Poole, England); and smooth muscle actin (SMA) mouse monoclonal antibody (α-SMA, 1:2000 dilution; Sigma). No significant difference was noted between the 2 c-Kit antibodies used. The concentrations of all antibodies used were determined by a series of titration experiments, which generally ranged from 1:50 to 1:6400. Immunoreactivity was demonstrated by incubating the tissues with primary antibodies (overnight, 4°C). Bound antibodies were visualized by incubation of tissues for 2 hours with either indocarbocyanine (Cy3)-, indocarbocyanine (Cy5)-, indocarbocyanine (Cy2)-, or lissamine rhodamine (LRSC)-labeled secondary antibodies to rabbit or mouse immunoglobulin (Ig) G (Jackson ImmunoResearch, West Grove, PA) diluted 1:100 (Cy2, LRSC) and 1:200 (Cy3, Cy5). After they were washed with PBS, the sections were mounted on slides, air-dried overnight at room temperature, then coverslipped. In some experiments, double-labeling immunohistochemistry was used to identify the relationship between ICC and either nerves or smooth muscle cells. Double labeling was made possible by use of primary antibodies raised in different species in conjunction with species-specific secondary antibodies (donkey, anti-mouse, anti-goat, and anti-rabbit; Jackson ImmunoResearch) coupled to contrasting fluorophores (Cy3, Cy5, Cy2, or LSRC). Nonspecific labeling for c-Kit, PGP 9.5, and α-SMA was checked by omitting the respective primary antibody. Specificity of labeling for c-Kit, PGP 9.5, and α-SMA was checked by preabsorption with the appropriate pure antigen. No labeling was observed with any of the antibodies with preabsorption of the appropriate pure antigen. Also, there was no staining when nonimmune serum was used instead of antibodies.

Volume Determination of ICC and Neural Networks

Immunostained tissues were examined with a laser scanning confocal microscope (Zeiss 310, Oberkochen, Germany). Cy3 and LSRC fluorescence was visualized using an Argon/Krypton ion laser at 568 nm for excitation and emission taken over 590 nm. Cy2 fluorescence was visualized using an Argon/Kryton ion laser tuned to 488 nm, and emission taken at 515/545. Cy5 fluorescence was visualized using a helium/neon ion laser at 633 nm emission taken above 670 nm.

Each specimen examined was divided into 4 anatomic regions: longitudinal muscle, myenteric plexus region, circular muscle, and submucosal border. Images were collected using an oil-immersion 40× objective (NA 1.3) and an oil-immersion 100× objective (NA 1.3). The 100× objective was used to ensure that weakly stained ICC were included in the quantitative analyses. In every region, 4 adjacent areas in the X–Y plane were examined. Under the 40× oil objective, the maximum area scanned in the horizontal X–Y plane was 320 μm × 320 μm; under the 100× oil objective, the area scanned was 128 μm × 128 μm. Optical sections (512 × 512 pixels) were recorded at 0.5-μm depth (optical *z* axis) increments through each of the 4 adjacent areas. Typically, 20 optical sections were obtained in each of the 4 areas and stored. The volume (in μm^3) of total tissue (including interstitial space) was calculated using the following formula: Area of X–Y Plane (μm^2) × (Number of Optical Sections −1) × 0.5(Distance Between Top of 2 Adjacent Sections). The volumes obtained from each of the 4 adjacent areas were combined and averaged. No obvious holes or tears caused by tissue preparation were present in the areas studied.

The volume occupied by ICC was calculated as follows. Files of the stored confocal images were transferred to either a Silicon Graphics Indy workstation (Mountain View, CA) or a SUN Microsystems SPARC station 2 workstation (Mountain View, CA) running on ANALYZE software (Mayo Foundation, Rochester, MN). Files were changed to ANALYZE format and converted into a 3-dimensional (3-D) data set by application of a 3-way interpolation algorithm. The gray scale data set was reconstructed in 3-D using volume rendering and appropriate thresholds to remove background noise. To avoid overthresholding, less intensely fluorescent structures such as the fine processes in ICC networks, the threshold value was slowly increased, eliminating voxels containing noise. As fine processes emerged, they were stored in an object file. The threshold was again increased until all visible processes were extracted. In double-labeling experiments, a gray scale data set was obtained for each fluorescent signal. The resulting images were merged using image algebra. A surface-shading algorithm was used to emphasize ICC surface features. The volume of the ICC network was obtained directly from the volume data set after mathematical correction for focal anomaly.[23] To correct for this distortion, measurements were made of the lateral and axial diameters of fluorescent beads (normal diameter, 10 μm; Fluorospheres; Coulter Corp., Hialeah, FL) under similar conditions as tissues. The beads contained either fluorescein or indocarbocyanine, and they were imaged with the same wavelengths and filter set used for the fluorescently tagged secondary antibodies. A similar procedure was used to calculate neuronal structure volume; for neuronal structures, only the circular muscle layer was examined.

Statistics

Data are presented as means ± SE. Statistical differences among different regions were tested using analysis of variance (ANOVA). *P* values of <0.05 were considered statistically significant.

Results

Demographics

The demographics of the patients with slow-transit constipation are shown in Table 1, and the demographics of the controls are shown in Table 2. All patients had at least a 10-year history of constipation, often dating back to childhood. All patients had prolonged colonic transit times as measured by a radionucleotide transit test, and conventional medical therapy had failed in all. All patients had normal rectal balloon expulsion test results to screen for pelvic floor dysfunction. The rectosphincteric reflex was present in all patients, excluding Hirshsprung's disease. All patients had normal barium enema or colonoscopy results within 1 year of surgery to exclude structural lesions.

ICC Distribution and Volume in Normal Sigmoid Colon

ICC were found in all layers of the sigmoid colon muscularis propria (Figure 1). A dense network of ICC was present at the level of the myenteric plexus, and a large number of ICC were present throughout the circular muscle layer. c-Kit–positive immunoreactive structures occupied 5.5% ± 0.7% of the total longitudinal muscle layer volume, 21.3% ± 1.9% of the myenteric plexus region volume, 7% ± 1.3% of the circular muscle layer volume, and 10.0% ± 1.4% of the volume of the submucosal plexus region (Figures 2 and 3). PGP

Table 1. Patient Demographics

Patient	Age (*yr*)	Sex	Colonic transit (GC at 24 h; n = 1.6–3.8)	Duration of constipation (*yr*)	Pathology report
1	71	F	1.1	Lifelong	Colon mildly dilated, more so proximally; no microscopic abnormality
2	37	F	1.6	>20	Histologically unremarkable colon, ileum, and appendix
3	42	F	1.3	>15	Colon, ileum, and appendix without diagnostic abnormality
4	23	F	1.3	10	Histologically unremarkable colon, ileum, and appendix
5	42	F	1.4	Lifelong	Histologically unremarkable colon, ileum, and appendix
6	36	F	Prolonged	Lifelong	Histologically unremarkable colon, ileum, and appendix

GC, geometric center.

Table 2. Control Demographics

Control	Age (*yr*)	Sex	Disease requiring resection
1	73	M	Sigmoid cancer
2	76	F	Sigmoid cancer (in polyp)
3	60	F	Sigmoid cancer
4	42	F	Inactive diverticular disease
5	72	F	Rectal cancer
6	43	F	Rectal cancer
7	66	F	Sigmoid cancer
8	66	F	Inactive diverticular disease

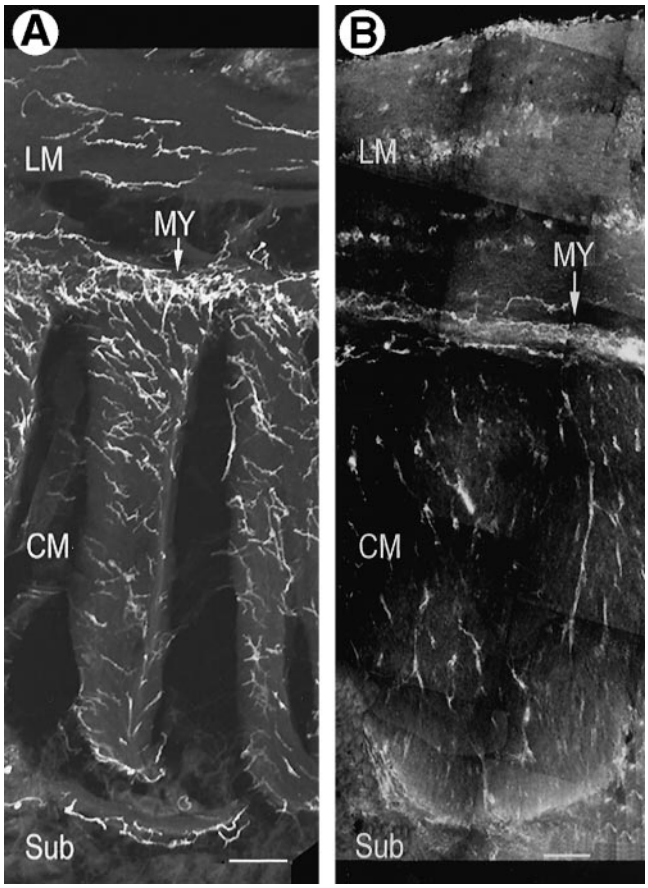

Figure 1. Overview of the distribution of ICC of Cajal (*A*) in normal human sigmoid colon and (*B*) in the sigmoid colon of a patient with slow-transit constipation. Each panel is made up of a montage of several fields of view. c-Kit–immunoreactive structures are shown in *white*. A decrease in c-Kit–positive immunoreactivity in all regions of the sigmoid colon is evident in *B* compared with *A*. Sections were cut parallel to the longitudinal muscle layer for both panels. LM, longitudinal muscle; MY, myenteric plexus region; CM, circular muscle; Sub, submucosal border. *Bars* = 100 μm.

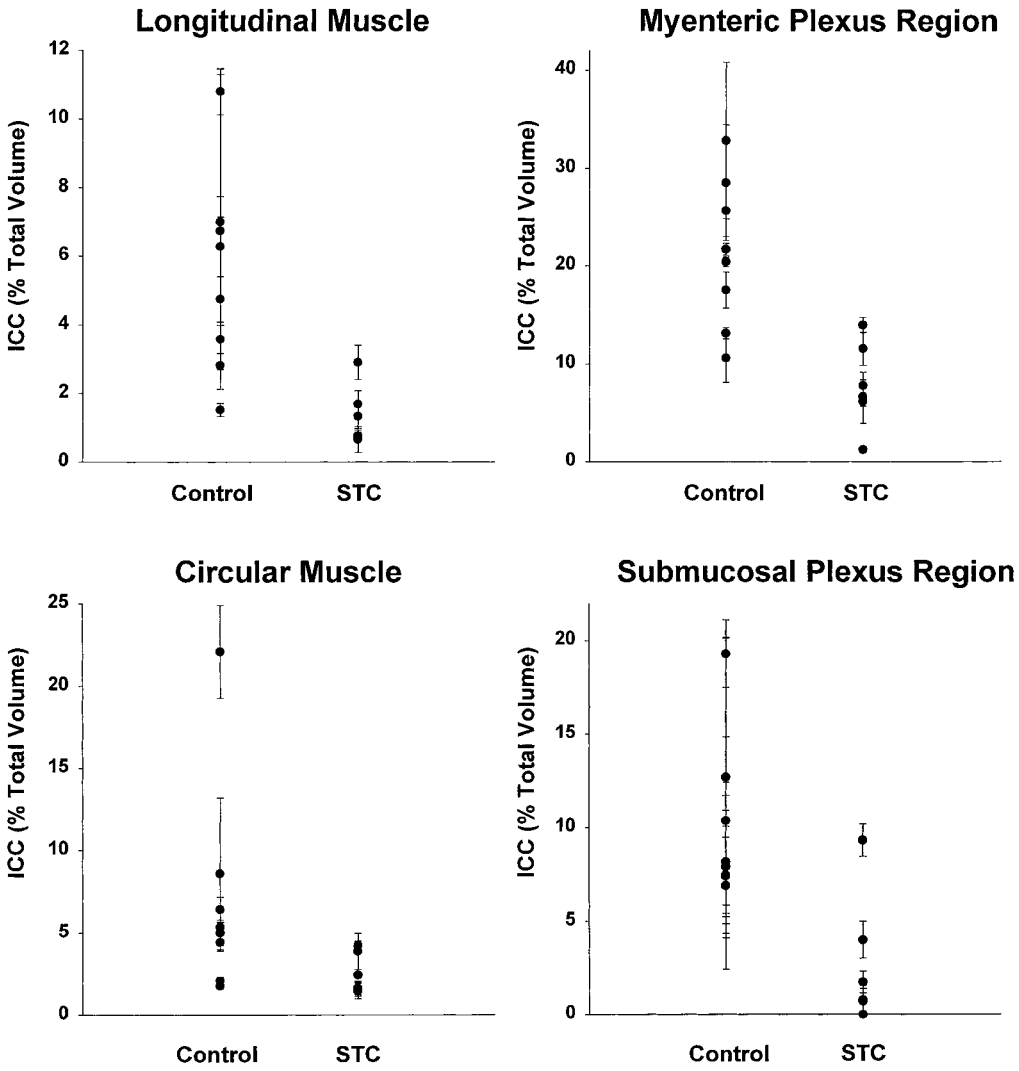

Figure 3. Scatter plots showing the percent volume occupied by ICC in the different regions of the sigmoid colon for each subject (STC, slow-transit constipation). Each point represents the mean ± SEM of 4 areas analyzed for each region. $P < 0.05$ (controls vs. STC) for all 4 regions.

9.5–positive structures occupied 18% ± 2.9% of the total volume of the circular muscle layer (Figure 2).

ICC Distribution and Volume in the Sigmoid Colon of Constipated Patients

ICC were present in all layers of the sigmoid colon, but their number was significantly reduced in each layer (Figure 1). c-Kit–positive immunoreactive structures occupied 1.5% ± 0.2% of the total longitudinal muscle layer volume, 7.9% ± 1% of the myenteric plexus region volume, 2.5% ± 0.3% of the circular muscle layer volume, and 2.8% ± 0.7% of the volume of the submucosal plexus region (all $P < 0.05$ compared with controls; Figures 3 and 4).

Microscopic examination of the remaining ICC in the slow-transit constipation group showed that at the level of single ICC, processes appeared to be blunted compared with processes from ICC visualized in normal controls (Figure 5).

Neuronal structures were also reduced in the sigmoid colons of patients with slow-transit constipation, and 7.7% ± 1.1% of the total circular muscle volume was positive for PGP 9.5 ($P < 0.05$ compared with controls; Figure 4). α-SMA staining did not show any evidence for smooth muscle hypertrophy in any of the specimens examined.

Discussion

The cause of constipation, even in patients with severe slow-transit constipation requiring surgery, is often elusive. The data presented in this report suggest that in addition to a previously described defect in innervation,[5–9] which the present study confirms, there is also a decrease in ICC volume. It is now established that ICC are required for generation of the smooth muscle electrical slow wave.[11,12] The electrical slow wave determines smooth muscle contractile activity. In the absence of an electrical slow wave, contractile activity is decreased and irregular, resulting in decreased intestinal transit.[13] The electrical slow wave in the colon appears to be generated by submucosal ICC.[24] A decrease in submuco-

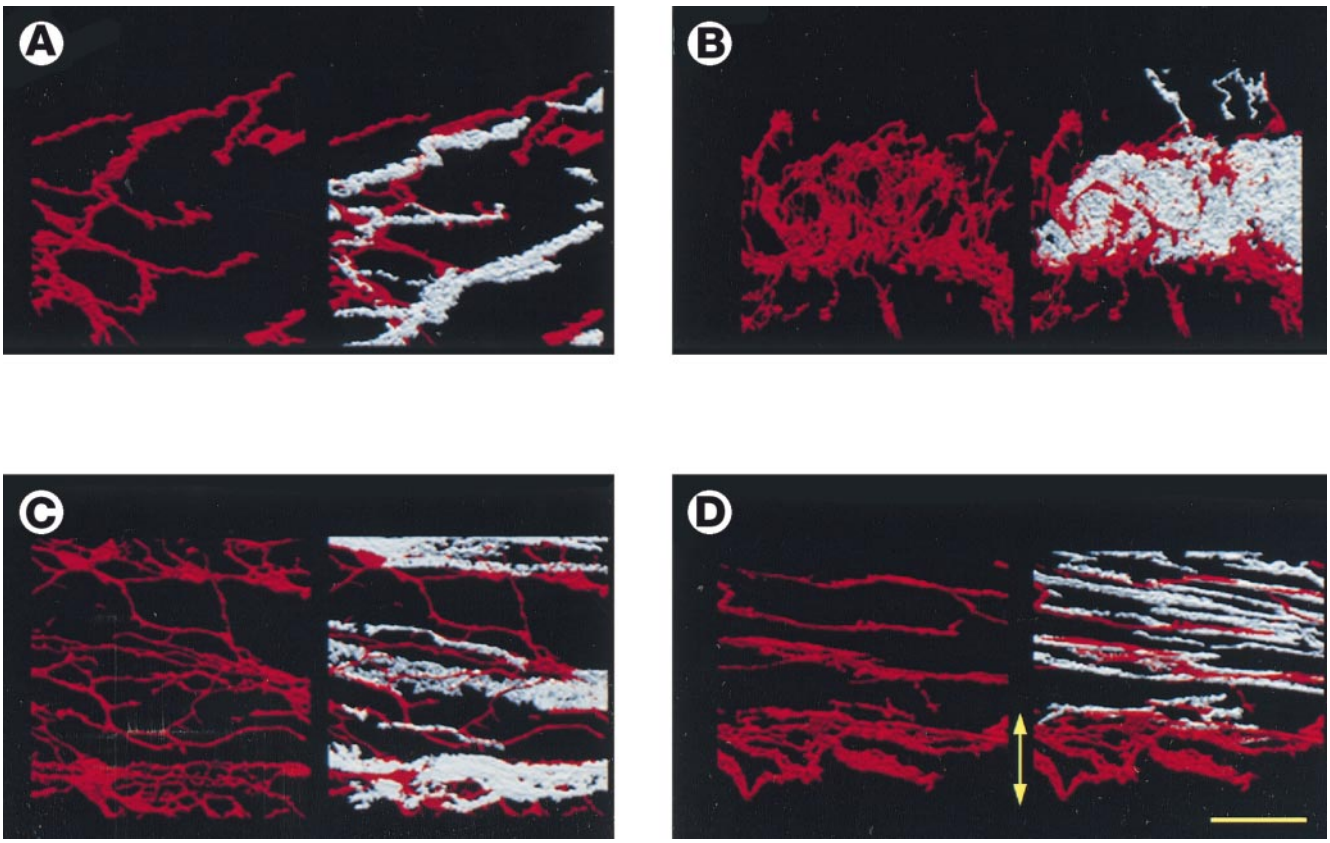

Figure 2. Distribution of ICC and neuronal structures in the normal human sigmoid colon. (*A*) Longitudinal muscle layer; (*B*) myenteric plexus region; (*C*) circular smooth muscle layer; (*D*) submucosal border (*yellow double arrow*). c-Kit–positive immunoreactivity is shown in *red* and PGP 9.5–positive immunoreactivity in *gray. Bar* = 50 μm.

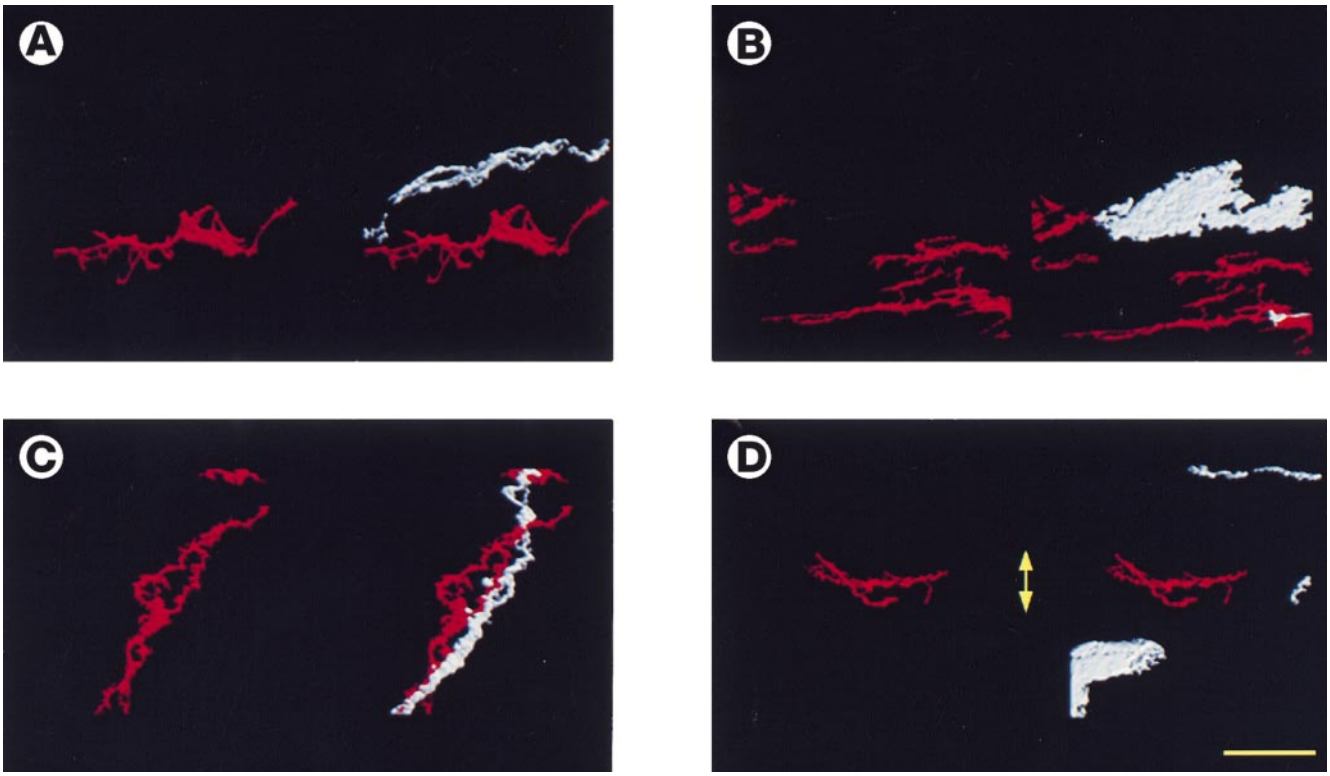

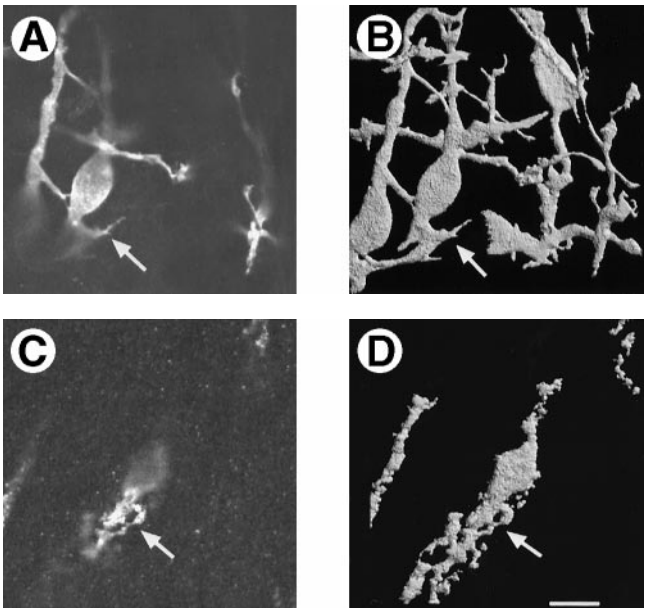

Figure 5. High-magnification view of ICC in the circular muscle layer. (*A*) Single slice obtained from normal human sigmoid colon; (*B*) reconstruction of 20 consecutive slices at 0.5-μm depth increments (*z*-axis). Note the fine processes of the individual ICC (*arrow*). (*C* and *D*) Similar data from human sigmoid colon of a patient with slow-transit constipation. Note the irregular surface markings and the loss of fine processes (*arrow*). *Bar* = 10 μm.

sal ICC, as shown in the present report, may lead to abnormal slow wave activity and decreased smooth muscle contractile activity, resulting in slow-transit constipation. ICC have also been suggested to act as transducers and amplifiers of neuronal signals to smooth muscle cells.[25,26] The significant decrease in ICC noted throughout the sigmoid colon in colonic specimens from patients with slow-transit constipation suggests that interactions between nerves and ICC and between ICC and smooth muscle would also be affected by the loss of ICC in the myenteric plexus region and smooth muscle layers. This would again be expected to disrupt normal colonic motility.

Use of 3-D techniques to quantify ICC volume offers several advantages over conventional cell counting techniques. The technique allows correct measurement of both cell bodies and cell processes. When counting cell bodies, it is possible to miss changes in cell body size or in cell processes. 3-D reconstruction also allows ICC volume to be determined from areas in which ICC density is too great to make out individual cells, such as in the myenteric plexus region.[27] Appropriate thresholding techniques allow information to be obtained from structures with varying or faint fluorescent signals.

On analysis of the reconstructed tissue sections, it appeared that in the slow-transit constipation group, the remaining ICC and neuronal structures often paralleled one another. It seems that areas in which one cell type (ICC or nerves) was lost also showed loss of the other cell type. The relationship between nerves and ICC remains unclear. In Sl/Sld mice that do not produce membrane-bound stem cell factor, the ligand for Kit, small intestinal ICC at the level of the myenteric plexus are largely absent, suggesting that stem cell factor is necessary for their development.[28,29] The major source of stem cell factor appears to be enteric neurons.[30,31] This would suggest that a primary deficit in enteric neurons secreting stem cell factor results in a decreased number of ICC. However, in contrast, in c-Ret knockout mice, which do not develop an enteric nervous system, ICC develop normally,[32,33] suggesting that nerves are not required for the development or maintenance of ICC. Also in W/W^V mutant mice, the small intestinal myenteric plexus appears to be normal, suggesting that ICC are not required for its development or maintenance.

The distribution and density of ICC for the normal sigmoid colon reported in this study differ from those of a recent study showing that ICC were less readily visible in standard histological sections.[34] Possible reasons for this discrepancy include the routine use in the present study of a 100× magnification lens to pick up faintly staining c-Kit–positive structures, use of computer algorithms to correctly threshold digitized images, and the method of preservation of specimens. All specimens studied in the current report were snap-frozen and stored at −70°C. In contrast, paraffin-embedded specimens were used in the previous study, necessitating reactivation of the c-Kit antigen. We have found (unpublished observations) that use of paraffin-embedded human colonic material results in an underrepresentation of c-Kit–positive structures.

In all patients with slow-transit constipation who require subtotal colectomy for treatment of constipation, medical therapy has failed, including use of laxatives. Before evaluation at a motility referral center, patients often use several over-the-counter laxatives including anthraquinone-containing laxatives. Anthraquinone-containing laxatives have been suggested to cause degen-

Figure 4. Distribution of ICC and neuronal structures in human sigmoid colon from a patient with slow-transit constipation. (*A*) Longitudinal muscle layer; (*B*) myenteric plexus region; (*C*) circular smooth muscle layer; (*D*) submucosal border (*yellow double arrow*). c-Kit–positive immunoreactivity is shown in *red* and PGP 9.5–positive immunoreactivity in *gray*. Note the decreased number of immunoreactive structures for both c-Kit (ICC) and PGP 9.5 (neuronal structures). *Bar* = 50 μm.

erative changes to colonic neuronal tissue.[35] If present, it is possible that a similar toxic effect may affect ICC, resulting in a decrease in number of ICC at the submucosal border. However, use of anthraquinone-containing laxatives would not be expected to alter ICC in other regions of the colon. Furthermore, recent publications suggest that anthraquinones do not cause degeneration of neuronal tissue.[36] It is unknown whether this finding can be extrapolated to ICC.

The present study used antibodies to c-Kit to quantify ICC. The c-Kit receptor is also found on mast cells. In a study of 2 patients with a myopathic form of chronic intestinal pseudo-obstruction, mast cells appear to account for less than 8% of the total c-Kit–positive cells in the gastrointestinal tract.[19] Mast cells are round and unlike ICC do not have processes, making their identification relatively easy. It is therefore highly unlikely that the findings in this article are secondary to changes in colonic mast cell content. A decrease in expression of c-Kit on ICC in patients with slow-transit constipation may result in overestimation of the decrease in the volume of ICC in colonic tissue from patients with slow-transit constipation. The use of a high numeric aperture, a high-magnification lens to collect data, and appropriate thresholding techniques makes this possibility less likely. Electron microscopy would be expected to provide a more definitive answer to this question. However, human colonic myenteric ICC seem to have a different electron micrographic appearance than myenteric colonic ICC from other species, making definitive identification difficult at present.[37,38] We have had the opportunity to examine 2 of the 6 slow-transit constipation specimens at electron microscopic level (unpublished observations). Although ICC appeared to be less abundant at the submucosal border, a region where human colonic ICC can be identified at the electron microscopic level, ICC volume and numbers were not quantified because of the smaller fields of view.

In summary, the present results suggest a possible etiological role for ICC in the pathogenesis of severe slow-transit constipation. It is not currently feasible for most pathology laboratories to accurately determine the 3-D volume of ICC in every resected colonic specimen or in full-thickness biopsy specimens. However, the marked decrease in ICC volume observed in the current report suggests that an assessment of ICC volume in future clinical studies might be warranted. Such an approach, applied to a large number of specimens, may shed more light on the pathophysiology of an incompletely understood disease process.

References

1. Brown DM, Everhart JE. Cost of digestive diseases in the United States. In: Everhart JE, ed. Digestive diseases in the United States: epidemiology and impact. US Department of Health and Human Services, Public Health Service, National Institutes of Health, National Institute of Diabetes and Digestive and Kidney Diseases. Washington, DC: US Government Printing Office, 1994, NIH publication 94–1447.
2. Surrenti E, Rath DM, Pemberton JH, Camilleri M. Audit of constipation in a tertiary referral gastroenterology practice. Am J Gastroenterol 1995;90:1471–1475.
3. Voderholzer WA, Schatke W, Muhldorfer BE, Klauser AG, Birkner B, Muller-Lissner SA. Clinical response to dietary fiber treatment of chronic constipation. Am J Gastroenterol 1997;92:95–98.
4. Nyam DC, Pemberton JH, Ilstrup DM, Rath DM. Long-term results of surgery for chronic constipation. Dis Colon Rectum 1997;40:273–279.
5. Krishnamurthy S, Schuffler MD, Rohrmann CA, Pope CE Jr. Severe idiopathic constipation is associated with a distinctive abnormality of the colonic myenteric plexus. Gastroenterology 1985;88:26–34.
6. Schouten WR, ten Kate FJ, de Graaf EJ, Gilberts EC, Simons JL, Kluck P. Visceral neuropathy in slow transit constipation: an immunohistochemical investigation with monoclonal antibodies against neurofilament. Dis Colon Rectum 1993;36:1112–1117.
7. Sjolund K, Fasth S, Ekman R, Hulten L, Jiborn H, Nordgren S, Sundler F. Neuropeptides in idiopathic chronic constipation (slow transit constipation). Neurogastroenterol Motil 1997;9:143–150.
8. Cortesini C, Cianchi F, Infantino A, Lise M. Nitric oxide synthase and VIP distribution in enteric nervous system in idiopathic chronic constipation. Dig Dis Sci 1995;40:2450–2455.
9. Tzavella K, Riepl RL, Klauser AG, Voderholzer WA, Schindlbeck NE, Muller-Lissner SA. Decreased substance P levels in rectal biopsies from patients with slow transit constipation. Eur J Gastroenterol Hepatol 1996;8:1207–1211.
10. Faussone-Pellegrini MS, Infantino A, Matini P, Masin A, Mayer B, Lise M. Neuronal anomalies and normal muscle morphology at the hypomotile ileocecocolonic region of patients affected by idiopathic chronic constipation. Histol Histopathol (in press).
11. Huizinga JD, Thuneberg L, Kluppel M, Malysz J, Mikkelsen HB, Bernstein A. W/kit gene required for interstitial cells of Cajal and for intestinal pacemaker activity. Nature 1995;373:347–349.
12. Ward SM, Burns AJ, Torihashi S, Sanders KM. Mutation of the proto-oncogene c-Kit blocks development of interstitial cells and electrical rhythmicity in murine intestine. J Physiol 1994;480:91–97.
13. Der-Silaphet T, Malysz J, Hagel SL, Arsenault A, Huizinga JD. Interstitial cells of Cajal direct normal propulsive contractile activity in the mouse small intestine. Gastroenterology 1998;114:724–736.
14. Vanderwinden JM, Liu H, De Laet MH, Vanderhaeghen JJ. Study of the interstitial cells of Cajal in infantile hypertrophic pyloric stenosis. Gastroenterology 1996;111:279–288.
15. Vanderwinden JM, Rumessen JJ, Liu H, Descamps D, De Laet MH, Vanderhaeghen JJ. Interstitial cells of Cajal in human colon and in Hirschsprung's disease. Gastroenterology 1996;111:901–910.
16. Yamataka A, Ohshiro K, Kobayashi H, Fujiwara T, Sunagawa M, Miyano T. Intestinal pacemaker C-KIT+ cells and synapses in allied Hirschsprung's disorders. J Pediatr Surg 1997;32:1069–1074.
17. Yamataka A, Kato Y, Tibboel D, Murata Y, Sueyoshi N, Fujimoto T, Nishiye H, Miyano T. A lack of intestinal pacemaker (c-Kit) in aganglionic bowel of patients with Hirschsprung's disease. J Pediatr Surg 1995;30:441–444.

18. Yamataka A, Ohshiro K, Kobayashi H, Lane GJ, Yamataka T, Fujiwara T, Sunagawa M, Miyano T. Abnormal distribution of intestinal pacemaker (C-KIT-positive) cells in an infant with chronic idiopathic intestinal pseudoobstruction. J Pediatr Surg 1998;33:859–862.
19. Isozaki K, Hirota S, Miyagawa J, Taniguchi M, Shinomura Y, Matsuzawa Y. Deficiency of c-kit+ cells in patients with a myopathic form of chronic idiopathic intestinal pseudo-obstruction. Am J Gastroenterol 1997;92:332–334.
20. Kenny SE, Vanderwinden JM, Rintala RJ, Connell MG, Lloyd DA, Vanderhaegen JJ, De Laet MH. Delayed maturation of the interstitial cells of Cajal: a new diagnosis for transient neonatal pseudo-obstruction. Report of two cases. J Pediatr Surg 1998;33:94–98.
21. Rumessen JJ. Ultrastructure of interstitial cells of Cajal at the colonic submuscular border in patients with ulcerative colitis. Gastroenterology 1996;111:1447–1455.
22. Lu G, Qian X, Berezin I, Telford GL, Huizinga JD, Sarna SK. Inflammation modulates in vitro colonic myoelectric and contractile activity and interstitial cells of Cajal. Am J Physiol 1997;273: G1233–G1245.
23. Visser TD, Oud JL, Brakehoff GJ. Refractive index and axial distance measurement in 3-D microscopy. Optik 1992;90: 17–19.
24. Smith TK, Reed JB, Sanders KM. Origin and propagation of electrical slow waves in circular muscle of canine proximal colon. Am J Physiol 1987;252:C215–C224.
25. Rumessen JJ, Thuneberg L. Pacemaker cells in the gastrointestinal tract: interstitial cells of Cajal. Scand J Gastroenterol 1996; 216(suppl):82–94.
26. Sanders KM. A case for interstitial cells of Cajal as pacemakers and mediators of neurotransmission in the gastrointestinal tract. Gastroenterology 1996;111:492–515.
27. Burns AJ, Herbert TM, Ward SM, Sanders KM. Interstitial cells of Cajal in the guinea-pig gastrointestinal tract as revealed by c-Kit immunohistochemistry. Cell Tissue Res 1997;290:11–20.
28. Ward SM, Burns AJ, Torihashi S, Harney SC, Sanders KM. Impaired development of interstitial cells and intestinal electrical rhythmicity in steel mutants. Am J Physiol 1995;269:C1577–C1585.
29. Mikkelsen HB, Malysz J, Huizinga JD, Thuneberg L. Action potential generation, Kit receptor immunohistochemistry and morphology of steel-Dickie (Sl/Sld) mutant mouse small intestine. Neurogastroenterol Motil 1998;10:11–26.
30. Torihashi S, Yoshida H, Nishikawa S, Kunisada T, Sanders KM. Enteric neurons express Steel factor-lacZ transgene in the murine gastrointestinal tract. Brain Res 1996;738:323–328.
31. Young HM, Torihashi S, Ciampoli D, Sanders KM. Identification of neurons that express stem cell factor in the mouse small intestine. Gastroenterology 1998;115:898–908.
32. Sanchez MP, Silos-Santiago I, Frisen J, He B, Lira SA, Barbacid M. Renal agenesis and the absence of enteric neurons in mice lacking GDNF. Nature 1996;382:70–73.
33. Schuchardt A, D'Agati V, Larsson-Blomberg L, Costantini F, Pachnis V. Defects in the kidney and enteric nervous system of mice lacking the tyrosine kinase receptor Ret. Nature 1994;367: 380–383.
34. Hagger R, Gharaie S, Finlayson C, Kumar D. Regional and transmural density of interstitial cells of Cajal in human colon and rectum. Am J Physiol 1998;275:G1309–G1331.
35. Tzavella K, Schenkirsch G, Riepl RL, Odenthal KP, Leng-Peschlow E, Muller-Lissner SA. Effects of long-term treatment with anthranoids and sodium picosulphate on the contents of vasoactive intestinal polypeptide, somatostatin and substance P in the rat colon. Eur J Gastroenterol Hepatol 1995;7:13–20.
36. Riecken EO, Zeitz M, Emde C, Hopert R, Witzel L, Hintze R, Marsch-Ziegler U, Vester JC. The effect of an anthraquinone laxative on colonic nerve tissue: a controlled trial in constipated women. Z Gastroenterol 1990;28:660–664.
37. Rumessen JJ, Peters S, Thuneberg L. Light and electron microscopical studies of interstitial cells of Cajal and muscle cells at the submucosal border of human colon. Lab Invest 1993;68:481–495.
38. Faussone-Pellegrini MS, Pantalone D, Cortesini C. Smooth muscle cells, interstitial cells of Cajal and myenteric plexus interrelationships in the human colon. Acta Anat 1990;139:31–44.

Received April 1, 1999. Accepted September 14, 1999.

Address requests for reprints to: Gianrico Farrugia, M.D., Mayo Clinic, Guggenheim 8, 200 First Street Southwest, Rochester, Minnesota 55905. e-mail: farrugia.gianrico@mayo.edu; fax: (507) 284-0266.

Supported by National Institutes of Health grants DK 52766 and 17238.

The authors thank Gary Stoltz and Adrian Holm for technical assistance and Kristy Zodrow for secretarial assistance.